

Ferromagnetic $0 - \pi$ Junctions as Classical Spins

M.L. Della Rocca,^{1,2,*} M. Aprili,^{1,3} T. Kontos,⁴ A. Gomez,¹ and P. Spatkis¹

¹*Ecole Supérieure de Physique et Chimie Industrielles (ESPCI), 10 rue Vauquelin, 75005 Paris, France*

²*Dipartimento di Fisica "E.R. Caianiello", Università degli Studi di Salerno, via S.Allende, 84081 Baronissi (Salerno), Italy*

³*CSNSM-CNRS, Bât.108 Université Paris-Sud, 91405 Orsay, France*

⁴*Institute of Physics, University of Basel, Klingelbergstrasse, 82, CH-4056 Basel, Switzerland*

(Dated: September 29, 2018)

The ground state of highly damped PdNi based $0 - \pi$ ferromagnetic Josephson junctions shows a spontaneous half quantum vortex, sustained by a supercurrent of undetermined sign. This supercurrent flows in the electrode of a Josephson junction used as a detector and produces a $\phi_0/4$ shift in its magnetic diffraction pattern. We have measured the statistics of the positive or negative sign shift occurring at the superconducting transition of such a junction. The randomness of the shift sign, the reproducibility of its magnitude and the possibility of achieving exact flux compensation upon field cooling: all these features show that $0 - \pi$ junctions behave as classical spins, just as magnetic nanoparticles with uniaxial anisotropy.

PACS numbers: 74.50.+r, 74.45.+j, 85.25.Cp

Macroscopic devices formed by a large number of particles can behave as a quantum two-level system provided phase coherence is conserved at the macroscopic scale [1, 2]. One example is the rf-SQUID, i.e. a superconducting ring interrupted by a Josephson junction. In a rf-SQUID quantum tunneling between two different macroscopic states corresponding to either zero or one quantum flux in the ring has been observed in the past [3, 4]. More recently, it was shown that when three Josephson junctions are introduced in the ring, the ground state is two-fold degenerate for an applied half quantum flux [5]. These two macroscopic configurations correspond to clockwise or anticlockwise circulating supercurrent. Coherent superposition between these two states has also been observed, making this device of great interest for quantum electronics [6, 7, 8]. However, as shown below, clockwise or anticlockwise circulating supercurrent can occur spontaneously (i.e. in zero applied magnetic field) when the three junctions in the ring are replaced by one π -junction (π -SQUID).

In this Letter, we show that the macroscopic ground state of a ferromagnetic Josephson junction shorted by a 0 weak link mimics that of a superconducting π -SQUID. Specifically, it is doubly degenerate, so that half a quantum vortex $\phi_0/2$ or half a quantum antivortex $-\phi_0/2$ appears in the junction. We investigate the classical limit of this two-level system, which behaves macroscopically as a magnetic nanoparticle of quantized flux, the magnetic anisotropy axis being defined by the junction plane.

π -junctions can be viewed as weak links characterized by an intrinsic phase difference across them equal to π [9, 10, 11, 12]. As a consequence, a π -junction in a superconducting loop is a phase bias generator that produces a spontaneous current and hence a magnetic flux [13]. In the limit $2\pi LI_c < \phi_0$, where I_c is the junction critical current and L is the self-inductance of the loop, the free energy is dominated by its magnetostatic

part and its minimum is reached for a zero total flux enclosed in the loop. The system maintains a constant phase everywhere and a shift of $\phi_0/2$ in the $I_c(\phi)$ relationship is expected [14, 15]. When $2\pi LI_c \gg \phi_0$, the Josephson part of the free energy dominates and a phase gradient throughout the loop favored thereby generating a spontaneous flux of $\pm\phi_0/2$. The spontaneous supercurrent can circulate clockwise and counterclockwise with exactly the same energy [13]. Applying a small magnetic field can lift this degeneracy and defines an easy magnetization direction. The existence of a spontaneous supercurrent sustaining half a quantum flux in π -rings has been recently shown in Nb loops interrupted by a ferromagnetic (PdNi) π -junction [16]. Direct scanning SQUID microscope imaging of the half-integer vortex has also been reported in HTSC grain boundary junctions [17, 18]. Analogously, a highly damped single Josephson junction fabricated with a 0 and a π region in parallel should display a spontaneous half quantum vortex at the $0 - \pi$ boundary [13].

We detect a spontaneous supercurrent by measuring the phase gradient with another Josephson junction. The ferromagnetic junction (source) and the detection junction (detector) are coupled, as shown in Fig.1(a), by sharing an electrode. I.e., the top electrode of the conventional Josephson junction is simultaneously the bottom electrode of the ferromagnetic one. If half a quantum vortex is spontaneously generated in the ferromagnetic junction, the spontaneous supercurrent that sustains it circulates in the common electrode [Nb2, Fig.1(a)] producing a phase variation equal to $\pi/2$. A $\phi_0/4$ -shift of the detection junction's diffraction pattern is thus produced. When an external magnetic field is applied, the diffraction pattern of the detection junction is given by:

$$I(B) = I(0) \frac{\sin \left[\frac{\pi}{\phi_0} (k_s J_s + k' \phi' + \phi) \right]}{\left[\frac{\pi}{\phi_0} (k_s J_s + k' \phi' + \phi) \right]} \quad (1)$$

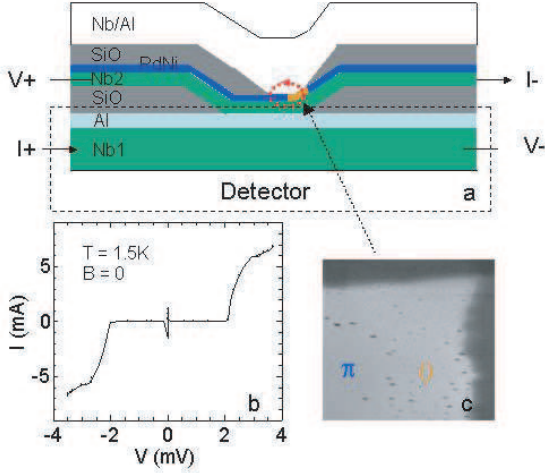


FIG. 1: (a) Schematic cross section of the device: a Nb based Josephson junction (detector) is coupled to a ferromagnetic (PdNi) junction (source) by sharing one electrode (Nb2). The red-colored closed loop indicates the half quantum vortex's location. (b) I-V characteristic of the detector at 1.5K in zero applied external field. (c) Scanning electron microscope image of the ferromagnetic junction edge area. The black spots are inhomogeneities which prevent PdNi continuity inducing a 0-coupling region.

where $\phi' = BDt'$ and $\phi = BDt$ are the magnetic fluxes through the ferromagnetic and detection junction respectively, with D the junction width, t and t' the effective barrier thickness. J_s is the spontaneous supercurrent density, $k_s = \frac{(\mu_0 \lambda_L(T)^2)}{2} D$ and $k' = \frac{(\mu_0 \lambda_L(T)^2)}{L} \frac{D}{w d_{Nb2}}$, with μ_0 the vacuum permittivity, $\lambda_L(T)$ the Nb London penetration depth, L the ferromagnetic junction inductance, w the junction length and d_{Nb2} the thickness of the common electrode, assumed to be of the order of the London penetration depth. The term $k_s J_s$ generates the shift due to the spontaneous supercurrent contribution, while the term $k' \phi'$ reduces the diffraction pattern period as a result of the contribution due to the screening current in the ferromagnetic junction.

Samples are fabricated by e-gun evaporation in an ultra high vacuum (UHV) system in a typical base pressure of 10^{-9} mbar. The whole device is fabricated completely in situ by shadow masks. The maximum degree of misalignment is $100 \mu\text{m}$. Deposition rates are monitored by a quartz balance with $0.1 \text{ \AA}/\text{s}$ resolution. First the bottom planar Nb/Al/Al₂O₃/Nb detection junction is made. A 1000 \AA thick Nb strip [Nb1, Fig.1(a)] is evaporated and backed by 500 \AA of Al. An Al₂O₃ oxide layer is achieved by oxygen plasma oxydation during 12 min, completed in a 10 mbar O₂ partial pressure during 10 min. A square window of $0.6 \times 0.8 \text{ mm}^2$ ($D \times w$), obtained by evaporating 500 \AA thick SiO layers, defines the junction area. Then, a 500 \AA thick Nb layer [Nb2, Fig.1(a)] is evaporated perpendicular to the Nb/Al strip to close the junction.

This procedure results in a junction critical temperature, T_{cj} , equal to 8.5K. Typical junction normal state resistances are of the order of $0.1 - 1 \Omega$ and critical current values are of $1 - 10 \text{ mA}$ at 4.2K. The resulting critical current density is $\sim 1 - 10^{-1} \text{ A/cm}^2$ leading to a Josephson penetration depth $\lambda_j \geq 1 \text{ mm}$, i.e. larger than the size of the junction (small limit). The I-V characteristic of a typical detector is shown in Fig.1(b). The Nb2 layer acts as both the counterelectrode of the bottom detection junction and the base electrode of the top ferromagnetic junction. Its thickness is comparable to the Nb penetration depth to insure good coupling between the two junctions. The same procedure is used to prepare the top planar Nb/PdNi/Nb/Al junction. Specifically, after defining the same junction area by evaporating 500 \AA thick SiO layers, a PdNi layer was evaporated directly on the Nb layer, without any Al-oxide barrier. This results in a very large critical current and very small junction resistance [19]. An estimate of the critical current density is $10^4 - 10^5 \text{ A/cm}^2$, so the Josephson penetration depth $\lambda_{jf} < 10^{-2} \text{ mm} \ll D$. Hence the "source" ferromagnetic junction is in the "large limit" with a large screening capability. The junction was closed by a 100 \AA thick Nb layer backed by a 750 \AA thick Al layer, resulting in a critical temperature, T_{cf} , of 3.6K. As the critical temperature of the detector was higher than that of the source, its diffraction pattern could be measured with and without spontaneous supercurrents. The Ni concentration was checked by Rutherford backscattering spectrometry on PdNi samples evaporated in the same run as the junctions and was equal to 9%, corresponding to an exchange energy, E_{ex} , of 10.5meV and a 0 to π -coupling transition for $d_{0-\pi} \sim 75 \text{ \AA}$.

An intrinsic feature of our fabrication technique is the formation of inhomogeneities at the window edges of the ferromagnetic junction [see Fig.1(c)]. SEM images and AFM analysis [20] have revealed bubbles [black spots in Fig.1(c)] with diameter of about $2 - 3 \mu\text{m}$ and roughness up to 1000 \AA much higher than the PdNi thickness. These inhomogeneities have been observed in all samples and they may produce shorts through the ferromagnetic layer resulting in a 0-coupling at the junction edge, independently from the PdNi layer thickness. Therefore, 0-junctions and $0 - \pi$ junctions are obtained with PdNi layer thickness corresponding to 0-coupling and π -coupling, respectively.

Measurements were made in a ⁴He flow cryostat. Residual fields were screened by cryoperm and μ -metal shields. All measurements showed comparable residual fields at 4.2K of some tenths of mG. Depending on the PdNi layer thickness, the ferromagnetic junction is either 0 or π while a spontaneous half quantum vortex or antivortex is expected only for π -coupling. This is the main result of our experiment as reported in Fig.2, where we show the diffraction patterns of three samples for PdNi thickness equal respectively to 40 \AA , 100 \AA and

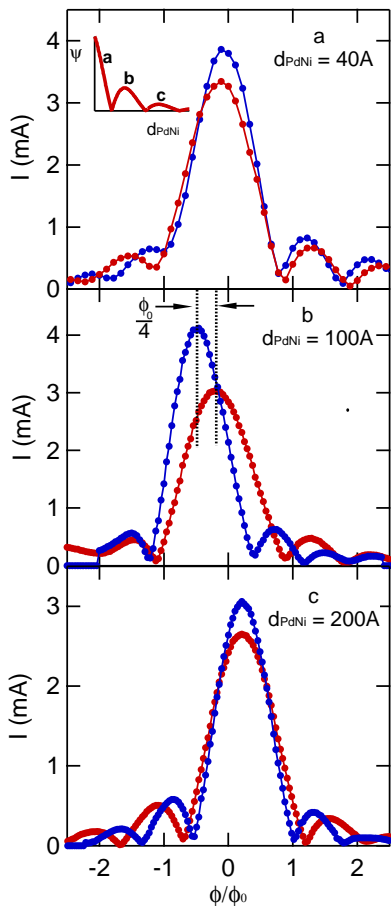


FIG. 2: Detector diffraction patterns for sources with $d_{PdNi} \sim 40\text{\AA} - 100\text{\AA} - 200\text{\AA}$, corresponding respectively to 0-coupling (a)–(c) and π -coupling (b). Measurements are taken at $T = 4.2\text{K} > T_{cf}$ (red data) and $T = 2\text{K} < T_{cf}$ (bleu data). A $\phi_0/4$ -shift of the maximum critical current appears in the (b) case, where a 0 - π coupling region is realized at the ferromagnetic junction edge. Inset: Oscillating behaviour of the order parameter as function of d_{PdNi} .

200\AA at $T = 4.2\text{K}$ (red data) and $T = 2\text{K}$ (bleu data). For 0-coupling [40\AA and 200\AA , Fig.2(a) and Fig.2(c) respectively] at $T < T_{cf}$, the period is reduced but no shift occurs in the detector diffraction pattern. The magnetic field corresponding to a quantum flux is 300mG. On the other hand, for π -coupling [100\AA , Fig.2(b)] the period reduction is accompanied by a shift of $\phi_0/4$ in the detector, as expected for a spontaneous half quantum vortex in the ferromagnetic junction. The period reduction at the lowest temperature (2K) for all the samples was about 15%. This value results from two competing effects: a smaller period is expected because of screening in the ferromagnetic junction as shown in eq.1, whereas the decrease in the penetration depth, $\lambda(T)$, at lower temperatures should increase the modulation period. We found no period reduction or diffraction pattern shift when the

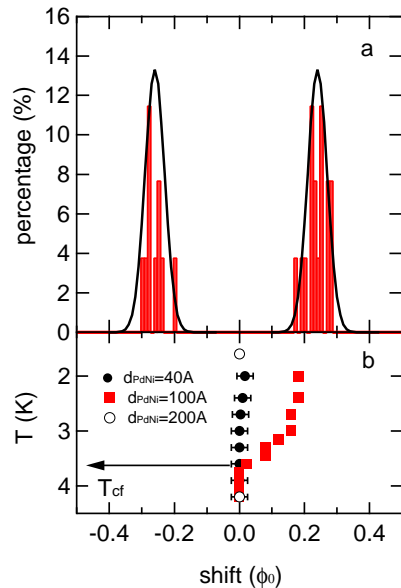


FIG. 3: (a) Amplitude histograms (red bars) of the spontaneous shift for 26 different cooldowns from room temperature of different samples, and their best Gaussian fits (black curves). The Gaussians have mean values of $+0.24\phi_0$ and $-0.26\phi_0$, with dispersions equal to $\pm 0.03\phi_0$. (b) Temperature dependence of the spontaneous shift for the samples of Fig.2: $d_{PdNi} \simeq 40\text{\AA}$ (black circles), $d_{PdNi} \simeq 100\text{\AA}$ (red square) and $d_{PdNi} \simeq 200\text{\AA}$ (open circles). The spontaneous half quantum flux appears below the ferromagnetic junction superconducting transition temperature, T_{cf} .

source and the detector were decoupled by a thin insulating layer. This indicates that ordinary inductive coupling between the two junctions is negligible. Regarding the possible effect of an external residual field or the magnetic layer itself on the spontaneous supercurrents, it is important to stress that the shifts are always about $\phi_0/4$ for π -coupling and zero for 0-coupling. Since this depends neither on the residual field nor, for 0-coupling, on the thickness of the ferromagnetic layer, any effect of the PdNi magnetic moment on the amplitude of the spontaneous supercurrents can be ruled out. The PdNi magnetic structure only lifts the degeneracy of the ground state and polarizes the supercurrents. As a consequence, the sign shift is always the same below the Curie temperature ($\sim 100\text{K}$), indicating the same spontaneous current polarization.

When cooling down from room temperature to 2K, the shift, while reproducible in magnitude, becomes random in sign as shown in Fig.3(a). The gaussian distribution functions used to approximate these distributions show mean values of $+0.24\phi_0$ and $-0.26\phi_0$ with equal dispersions of $\pm 0.03\phi_0$. This is the expected behavior of a two-fold degenerate ground state corresponding to either half a quantum flux or half a quantum antflux in the ferromagnetic junction. The same distribution would

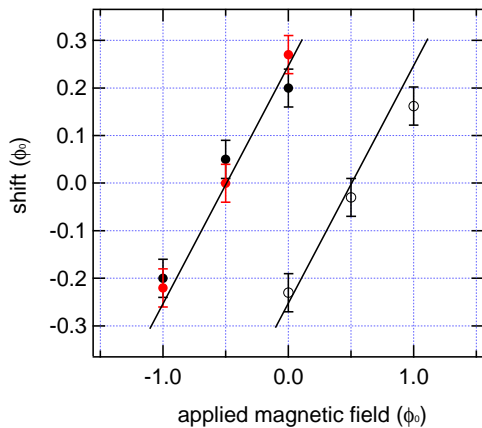


FIG. 4: Field cooled measurements for a half and an integer quantum flux applied to the ferromagnetic junction in the direction opposite to the spontaneous half quantum flux during cooldown through T_{cf} .

be expected for a magnetic nanoparticle with a significant uniaxial magnetic anisotropy. The large dispersion in shifts can be related to an intrinsic limit of the device itself since the same dispersion is observed when measuring devices with uniform 0 -coupling ferromagnetic junction, where the mean shift value is 0 . At 2K , the thermal activation energy ($K_b T \simeq 0.2\text{meV}$) is negligible with respect to the Josephson energy ($E_J = \frac{I_c \phi_0}{2\pi} \simeq 10^5 - 10^6 \text{eV}$ for $J_c \sim 10^4 - 10^5 \text{A/cm}^2$ and a junction area, $D \times w$, of 0.48mm^2) and hence no hopping between the two potential wells can occur. Fig.3(b) shows the temperature dependence of the shift measured for the junctions whose results are presented in Fig.2. A finite shift is observed starting from 3.6K (T_{cf}). The shift saturates at low temperature, just as the critical current does. Fig.3(b) also shows that the shift remains zero, as expected, for 0 -junctions.

Finally we studied the polarization of the spontaneous supercurrents when an external magnetic field is applied during cooling down through T_{cf} (Field-Cool (FC)). This field breaks time reversal symmetry and lifts the ground state degeneracy. In Fig.4 we show the diffraction pattern shift as a function of the applied flux for either a half- or an integer quantum flux in the ferromagnetic junction. For zero-field cooling (ZFC), the shift is either $+\phi_0/4$ (red and black circles) or $-\phi_0/4$ (open circles). When cooling occurs with a $\phi_0/2$ flux in the direction opposite to the spontaneous flux, screening currents in the ferromagnetic junction are induced, which compensate exactly for the half quantum vortex, so that no shift results. When cooling with a flux ϕ_0 in the direction opposite to the spontaneous flux, the screening current and the spontaneous ones add up, inducing a net flux equal to half a quantum in the direction opposite to the spontaneous one. The two lines, in Fig.4, define the slip-over from vortex to antivortex and vice-versa under FC.

In conclusion, we have probed the ground state of highly damped ferromagnetic $0 - \pi$ junctions by a phase sensitive technique. The samples were directly coupled to a detection junction with a higher critical temperature via a shared electrode. The spontaneous supercurrent, sustaining half a quantum vortex in the $0 - \pi$ junction, produced a $\phi_0/4$ -shift in the detection junction diffraction pattern below the ferromagnetic junction transition. Although equal in magnitude, the shifts were random in direction for different cooldowns, as a result of the doubly degenerate ground state of the $0 - \pi$ junction, corresponding to equal vortex or antivortex probabilities. Thus a $0 - \pi$ Josephson junction is a macroscopic realization of a two-level system and behaves in the classical limit as a single magnetic domain with uniaxial anisotropy. It would be interesting to investigate the quantum limit by reducing the temperature and the barrier height between the two potential wells.

We are indebted to A. Bauer and C. Strunk for suggesting the field-cooled compensation and E. Reinwald for performing a detailed AFM study on our samples. We also thank H. Pothier, A. Buzdin, E. Goldwin, J. Lesueur for stimulating discussions; S. Collin for technical assistance and H. Bernas for a critical reading of the manuscript. This work has been partially funded by ESF through the " π -shift" program.

* Electronic address: marilu@sa.infn.it

- [1] A.O. Caldeira and A.J. Leggett, *Ann.Phys.* **149**, 347, (1983).
- [2] A.J. Leggett et al, *Rev. Mod. Phys.* **59**, 1, (1987).
- [3] R.J. Prance et al., *Nature* **289**, 543, (1981).
- [4] D.B. Schwartz, B. Sen, C.n. Archie, and J.E. Lukens, *Phys. Rev. Lett.* **55**, 1547, (1985).
- [5] J.E. Mooij et al., *Science* **285**, 1036, (1999).
- [6] C.H. van der Wal et al., *Science* **290**, 773, (2000).
- [7] J.R. Friedman et al., *Nature* **406**, 43, (2000).
- [8] I. Chiorescu et al., *Science* **299**, 1869, (2003).
- [9] A.V. Andreev, A.I. Buzdin, and R.M. Osgood, *Phys. Rev. B* **43**, 10124, (1991).
- [10] A.I. Buzdin and M.Y. Kupriyanov, *JETP Lett.* **53**, 321, (1991).
- [11] T. Kontos et al., *Phys. Rev. Lett.* **89**, 137007, (2002).
- [12] V.V. Ryazanov et al., *Phys. Rev. B* **65**, 020501, (2001).
- [13] L.N. Bulaevskii, V.V. Kuzii, and A.A. Sobyenin, *Solide State Comm.* **25**, 1053, (1978).
- [14] W. Guichard et al., *Phys. Rev. Lett.* **90**, 167001, (2003).
- [15] R.R. Schulz et al., *Appl. Phys. Lett.* **76**, 912, (2000).
- [16] A. Bauer et al., *Phys. Rev. Lett.* **92**, 217001, (2004).
- [17] J.R. Kirtley et al., *Phys. Rev. Lett.* **76**, 1336, (1996).
- [18] J.R. Kirtley, C.C. Tsuei, and K. A. Moler, *Science* **285**, 1373, (1999).
- [19] H. Sellier, C. Baraduc, F. Lefloch, and R. Calmcsuk, *Phys. Rev. B* **68**, 054531, (2003).
- [20] M. Aprili et al., *Proceeding of NATO Advanced Research Workshop on Nanoscale Devices - Fundamentals and Applications*, Kishinev, Moldavia (2004).